Precambrian Research 238 (2013) 199–213

Contents lists available at ScienceDirect

Precambrian Research

journal homepage: www.elsevier.com/locate/precamres

Re–Os age constraints and new observations of Proterozoic glacial deposits in the Vazante Group, Brazil

Nicholas J. Geboy[a,*], Alan J. Kaufman[b,c], Richard J. Walker[b], Aroldo Misi[d], Tolentino Flavio de Oliviera[e], Kristen E. Miller[f], Karem Azmy[g], Brian Kendall[h], Simon W. Poulton[i]

[a] United States Geological Survey, Reston, VA 20192, USA
[b] University of Maryland, Department of Geology, College Park, MD 20742, USA
[c] University of Maryland, Earth System Science Interdisciplinary Center, College Park, MD 20742, USA
[d] Centro de Pesquisa em Geofísica e Geologia, Universidade Federal da Bahia (CPGG/UFBA), CEP 40170-290, Salvador, Bahia, Brazil
[e] Independent Consultant, Rio de Janeiro, RJ, Brazil
[f] Massachusetts Institute of Technology, Department of Earth, Atmospheric and Planetary Sciences, Cambridge, MA 02139, USA
[g] Department of Earth Sciences, Memorial University of Newfoundland, St. John's, Newfoundland A1B 3X5, Canada
[h] University of Waterloo, Department of Earth and Environmental Sciences, Waterloo, Ontario N2L 3G1, Canada
[i] University of Leeds, School of Earth and Environment, Leeds LS2 9JT, United Kingdom

ARTICLE INFO

Article history:
Received 26 March 2013
Received in revised form 22 August 2013
Accepted 10 October 2013
Available online xxx

Keywords:
Vazante Group
Mesoproterozoic glaciation
Re–Os geochronology
Fe-speciation

ABSTRACT

A new Re–Os radiometric age date for an organic-rich shale horizon from the Vazante Group in Brazil, coupled with geological observations, provide evidence for late Mesoproterozoic glacial episodes, conflicting with the general view of greenhouse conditions marked by a eustatic high stand at this time. Field observations of a reverse fault juxtaposing older Mesoproterozoic sedimentary rocks above younger Neoproterozoic strata provide a new stratigraphic framework and reconcile the apparent inversion of U–Pb detrital zircon ages through the succession. Combined, the geochronological, geochemical and stratigraphic evidence suggest that the Vazante Group sediments accumulated along a passive margin of the São Francisco craton and are correlative with the neighboring Paranoá Group. Biomarker, sulfur isotope and iron speciation analyses support the interpretation of a strongly stratified water column during post-glacial transgression and deposition of one of the bituminous shale horizons. The relationship of the glaciogenic Vazante Group to other late Mesoproterozoic successions, such as the non-glacial Atar Group in West Africa and Bylot Supergroup in arctic Canada, however, remains enigmatic.

Published by Elsevier B.V.

1. Introduction

The Precambrian geologic record contains evidence of widespread ice ages, including diamictite left behind by melting glaciers, capped by texturally and isotopically anomalous carbonate and organic-rich shale that accumulated in the wake of rising sea levels (Harland and Bidgood, 1959; Kaufman et al., 1991; Kirschvink, 1992; Kennedy, 1996; Hoffman et al., 1998; Schrag et al., 2002; Bekker et al., 2005). Existing age constraints suggest that these Precambrian ice ages were episodic rather than continuous, with a series of temporally discrete glaciation events occurring at the beginning and end of the Proterozoic Eon (*cf.* Kaufman et al., 1997; Kennedy et al., 1998; Walter et al., 2000; Kendall et al., 2004, 2006) but with little evidence of glaciation in the intervening billion years.

Due to the general lack of radiometric determinations on sedimentary successions, however, the absolute ages of many of the Proterozoic diamictites are poorly known. To advance understanding of the tempo and mode of these ancient ice ages, researchers have applied a geochronometer based on the radioactive decay of ^{187}Re to ^{187}Os, most commonly on samples of organic-rich shale preserved in drill cores (Kendall et al., 2004, 2006; Azmy et al., 2008; Rooney et al., 2010) or syn-depositional sulfide grains (Hannah et al., 2004). Published results for Neoproterozoic (1.0–0.542 Ga) successions support the view that the Sturtian and Marinoan glacial epochs represented multiple discrete ice ages over a protracted time frame (*cf.* Kaufman et al., 1997). Contrary to expectations, a Re–Os study of a dropstone-laden shale horizon from the Vazante Group in south-central Brazil (Azmy et al., 2008) indicated a late Mesoproterozoic age – a time previously believed to have been ice free.

* Corresponding author. Tel.: +1 703 648 6481.
E-mail address: ngeboy@usgs.gov (N.J. Geboy).

0301-9268/$ – see front matter. Published by Elsevier B.V.
http://dx.doi.org/10.1016/j.precamres.2013.10.010

In this paper, we re-evaluate the stratigraphic position of this shale, which was previously interpreted to be syn-glacial in origin (Olcott et al., 2005) and support the Mesoproterozoic age with new Re–Os work from a second shale horizon unrelated to glacial deposits, as well as identify a thrust fault lower in the Vazante Group that juxtaposes older Mesoproterozoic strata above younger glaciogenic sedimentary rocks of Neoproterozoic age. Detrital zircon U–Pb constraints for the Vazante Group (Rodrigues et al., 2012), coupled with carbon and strontium isotope data and paleontological evidence, are consistent with the stratigraphic inversion and our Re–Os age determinations.

2. Geologic and geochronologic background

The Vazante Group is a sedimentary succession that occurs in wide swaths atop the eastern part of the Brasília Fold Belt (BFB) on the western margin of the São Francisco craton throughout Minas Gerais, Brazil (Fig. 1). Surface outcrops are strongly weathered and the succession has been exposed to sub-greenschist facies metamorphism (Babinski et al., 2005; Azmy et al., 2008), but well preserved carbonate and organic-rich shale are available in drill core. Fig. 2 shows a generalized stratigraphy of the Vazante Group, including three potential glacial horizons, as well as the reverse fault located near the town of Lagamar (Pinho and Dardenne, 1994), which resulted in older strata of the Vazante Group – including the shale horizons studied here – to overly younger sedimentary rocks (see Section 5.1 for further details and implications). The basal Vazante diamictite (St. Antônio do Bonito Formation) has long been interpreted as glacial in origin based on the presence of faceted and striated cobbles of mixed lithology, including basement clasts, floating in a mudstone matrix (Dardenne, 2000). The two upper Vazante Group diamictites at the base of the Morro do Calcário and Lapa formations are characterized by carbonate breccia or laminated shale disrupted by carbonate dropstones. Further evidence for a glacial origin for the two upper Vazante diamictites includes: (1) their widespread distribution across the basin; (2) the observation that cobbles and boulders in the Morro do Calcário (previously attributed to the Serra do Poço Verde Formation) are both rounded and angular, with the rounded stones often faceted (Fig. 3A and B); (3) the thick black Morro do Calcário shale contains glendonite, a pseudomorph of ikaite, a carbonate mineral that forms in organic-rich sediment at temperatures between −1.9 and 7 °C (*cf.* Olcott et al., 2005); (4) the uppermost strata of the Lapa diamictite are Fe-oxide cemented with local accumulations of iron-formation (*cf.* Derry et al., 1992; Kaufman et al., 1997; Hoffman et al., 1998); and (5) the carbonates and marl overlying both diamictites preserve negative $\delta^{13}C$ excursions typical of post-glacial cap carbonates (Azmy et al., 2001, 2006; Brody et al., 2004).

The three shale horizons sampled for Re–Os analysis in this study were from, in ascending order, the pre-glacial Serra do Garrote Formation and the post-glacial Morro do Calcário and Lapa formations. The Serra do Garrote Formation consists of dark gray shale hundreds of meters thick that has been metamorphosed to a greenish slate in some areas; the shale can be carbonaceous and/or pyrite bearing (Dardenne, 2000). The Morro do Calcário and Lapa formations are both composed of laminated shale and dolostone, which contain intermittent ice-rafted debris and based on core observations are each several hundred meters thick (Dardenne, 2000). The true thickness of these units, however, is difficult to ascertain insofar as outcrops are discontinuous and coupled with the likelihood of tectonic repetition of strata due to thrust faulting. The Morro do Calcário and Lapa formations accumulated during post-glacial transgression over sub-glacial valleys largely filled with carbonate breccia. Sub-glacial unconformities cut through underlying carbonate platform deposits of the Serra do Poço Verde and Morro do Calcário formations (indicated by the heavier formation-boundary lines in Fig. 2); in some cores it appears that the two upper Vazante Group diamictites are in direct contact while in others they are separated by a variety of bedded lithologies.

The age of the Vazante Group is controversial. Cloud and Dardenne (1973) argued that the presence of the stromatolite *Conophyton metula Kirichenko* (Fig. 3C) near the base of the Lagamar Formation suggests an age ranging between 1350 and 950 Ma. Stromatolite biostratigraphy, however, is poorly constrained and competing tectonic models suggest a Neoproterozoic initiation of Vazante Group sedimentation either in a rapidly subsiding foreland basin associated with the Brasíliano collision (*ca.* 790 Ma; Dardenne, 2000) or along a passive continental margin during supercontinent breakup (*ca.* 900 Ma; Pimentel et al., 2001). Whole rock Rb–Sr data for a Vazante Group shale yielded an isochron age of ~600 Ma, but this age likely represents a date related to Brasíliano metamorphism (Amaral and Kawashita, 1967). A Neoproterozoic age for the upper Vazante Group was suggested based on a comparison of time-series isotope trends (Azmy et al., 2001), although an alternative interpretation of these variations suggested an older potential age for the succession (Misi et al., 2007). Most recently, Re–Os dates of 993 ± 46 and 1100 ± 77 Ma (excluding Re- and Os-poor samples) were determined from a dropstone-laden shale in the Vazante Group previously believed to be part of the Lapa Formation (Azmy et al., 2008) but here is assigned to the Morro do Calcário Formation (see below).

3. Methods

All samples were taken from two pristine drill cores provided by Votorantim Metais. For Re–Os analysis, samples were selected from the Serra do Garrote Formation in drill hole 134-86, from roughly coeval horizons of the Morro do Calcário Formation in drill holes 42-88 and 134-86 and from the Lapa Formation in drill hole 134-86. The upper two shale horizons in core 134-86 are separated by a thick interval of carbonate breccia, quartzite and iron-cemented diamictite (Brody et al., 2004). In 2009, we re-examined this core and concluded that the shale horizon Azmy et al. (2008) studied from drill hole MASW-01 belonged to the Morro do Calcário Formation, rather than the Lapa Formation as previously discussed.

3.1. Re/Os

The Re–Os system can provide precise depositional ages for organic-rich shale because these facies are often deposited in anoxic environments where Re and, to a lesser extent, Os may be sequestered from seawater in their reduced states and incorporated into organic matter (Ravizza and Turekian, 1989; Cohen et al., 1999; Selby and Creaser, 2003; Kendall et al., 2004). Once incorporated in the sediment, ^{187}Re undergoes beta decay to ^{187}Os with a half-life of approximately ~42 Ga. With the assumption that all of the shale samples in a suite have the same initial osmium isotopic composition (from coeval seawater) and a wide range in parent:daughter ratios, it is possible to generate an isochron, which yields the age of incorporation of Re and Os into the system and, hence, of deposition. Since shale facies contain both hydrogenous and terrigenous components, it is necessary to digest the samples with a less-aggressive medium, such as Cr^{VI}-H_2SO_4, which preferentially attacks the organic component while leaving the detrital quartz and feldspar largely intact (Selby and Creaser, 2003).

Approximately 50 mg of powdered whole rock was accurately weighed along with a known quantity of a ^{190}Os–^{185}Re spike and Cr^{VI}-H_2SO_4 digestion solution (Selby and Creaser, 2003) and transferred to frozen Carius tubes that were chilled using a mixture of

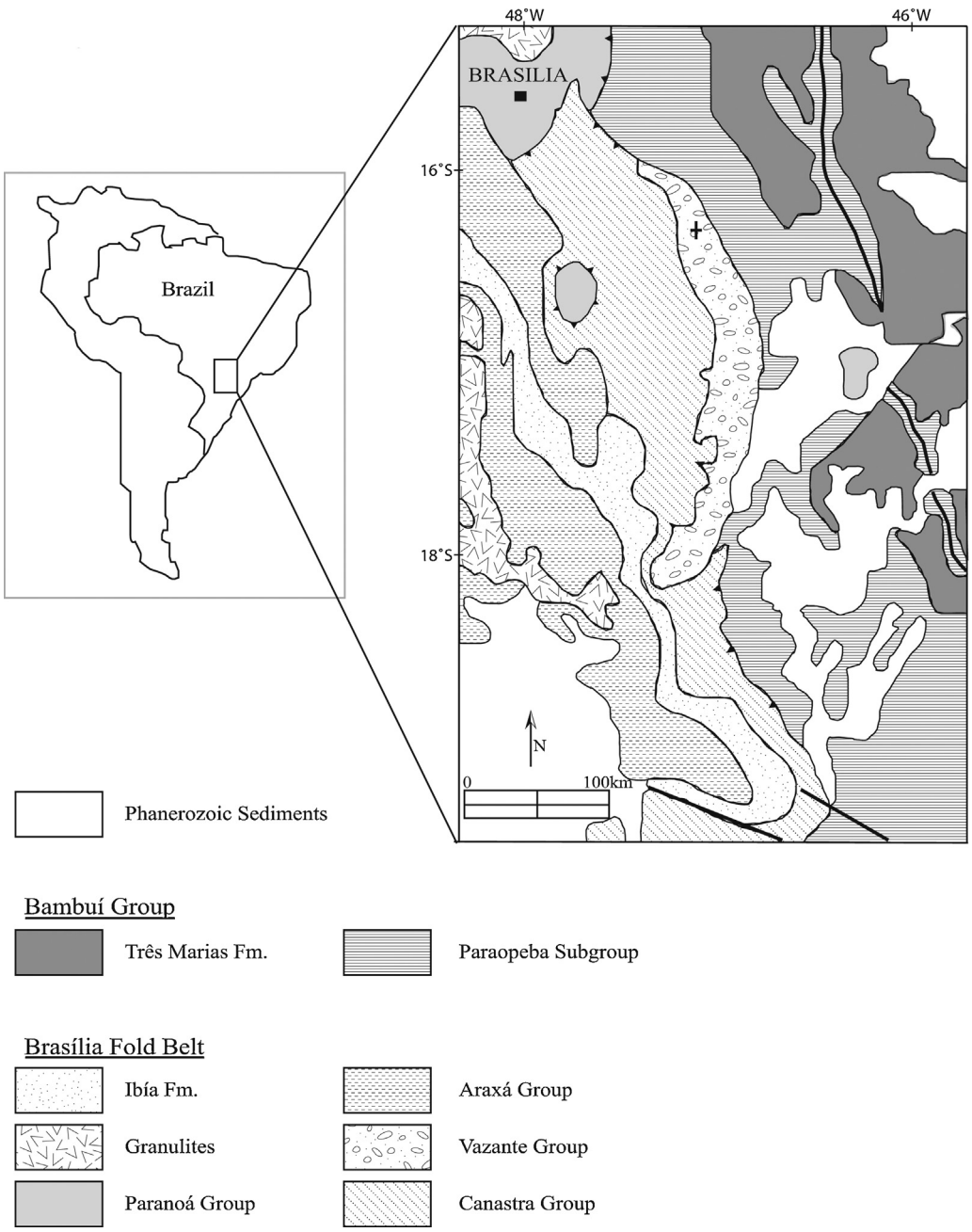

Fig. 1. Geologic map of study area. The Vazante Group is elongated north to south within Brazil with + indicating the approximate location of the drill cores examined here. Modified from Babinski et al. (2005).

dry ice and ethanol before being sealed with an oxy-propane torch (Shirey and Walker, 1995). Once thawed, the Carius tubes were placed in an oven heated to 240 °C for 48 h to fully oxidize the Re and Os to their highest valence states. Following digestion, the tubes were frozen in liquid nitrogen and opened. The Os was separated from the mixture via solvent extraction using carbon tetrachloride, back extracted into HBr and purified by micro-distillation prior to being loaded onto a Pt filament and analyzed using negative thermal ionization mass spectrometry (N-TIMS; Birck et al., 1997; Cohen and Waters, 1996). Following Os separation, the remaining solution was treated with sulfurous acid to reduce the Cr^{6+} to Cr^{3+}, and Re was separated using anion exchange chromatography before being taken up in 2% nitric acid and analyzed using inductively coupled plasma mass spectrometry (ICP-MS). All of the preparation chemistry and spectrometry were conducted at the University of Maryland's Geochemical Laboratories. Samples were blank corrected, with total analytical blanks averaging 19 pg and <1 pg for Re and Os, respectively. These blanks were sufficiently low as to have no effect on analytical uncertainties. Reproducibility was determined using a ^{185}Re spiked in-house standard of the Agpalilik iron meteorite, where $^{185}Re/^{187}Re = 1.331 \pm 0.002$ ($n = 10$; 2SDM) over a two-month measuring period and a UMD Os standard where $^{187}Os/^{188}Os = 0.1140 \pm 0.0003$ ($n = 9$; 2SDM) and $^{190}Os/^{192}Os = 1.981 \pm 0.002$ ($n = 9$; 2SDM) over a nine-month measuring period. Regressions were performed with *Isoplot V.4.15* (Ludwig, 2012) using a value of $1.666 \times 10^{-11}\,yr^{-1}$ for the ^{187}Re decay constant and 2σ uncertainties for $^{187}Re/^{188}Os$ and $^{187}Os/^{188}Os$ as determined by numerical error propagation.

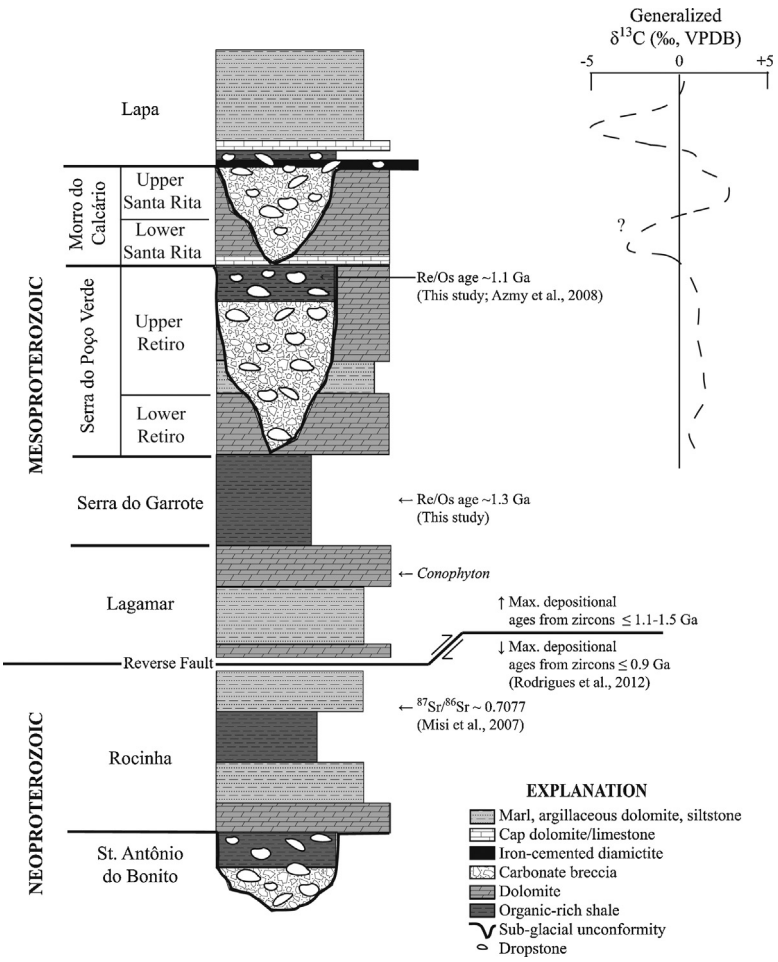

Fig. 2. Generalized stratigraphy of the Vazante Group with formation and member names highlighting sub-glacial valleys and post-glacial fill, the newly discovered reverse fault and geochronometric constraints discussed in the text. Modified after Dardenne (2000) with generalized C-isotope trends from Azmy et al. (2001, 2006). No vertical scale implied.

3.2. Total organic carbon and stable isotopes

Shale horizons were sampled from drill cores 134-86 and 42-88 for time-series analyses. Samples were ground with a ceramic mortar and pestle and aliquots were used for measuring total organic carbon (TOC) abundance, stable S and C isotope analyses, as well as Fe-speciation. TOC was determined using Dumas combustion techniques on pre-acidified powders and quantified on a vacuum distillation line. The $\delta^{13}C$ of the TOC was determined by combustion in a Eurovector elemental analyzer in-line with an Isoprime gas source isotope ratio mass spectrometer (EA-IRMS). Sulfide sulfur in the shales was isolated using a chrome-reduction solution (*cf.* Canfield et al., 1986) to release H_2S, which was carried in a stream of nitrogen gas through a Milli-Q ultrapure water trap to remove chloride. Sulfur was then trapped as Ag_2S with a 0.02 M solution of $AgNO_3$ and 1.55 M HNO_3. Silver sulfide solutions were set in the dark for approximately seven days, then filtered and rinsed with ~250 ml Milli-Q water and ~5 ml 1 N ammonia solution (NH_4OH). Samples were aged to allow for the dissolution of oxygen-bearing contaminants that precipitate with the silver sulfide. The black Ag_2S precipitate was then filtered and dried for ~48 h and combined with excess V_2O_5 in tin cups for EA-IRMS measurement of sulfur isotope compositions. Uncertainties of carbon and sulfur isotope analyses based on multiple analyses of urea and NBS-127 standards were better than 0.1 and 0.3‰, respectively.

3.3. Fe-speciation

Iron-speciation analyses, based on measured abundances of Fe in carbonate, oxide and sulfide mineral phases, as well as total Fe in samples, were conducted following procedures outlined by Poulton and Canfield (2005). Sulfide iron abundance (Fe–S) is calculated from Ag_2S yields in CRS extractions (see Section 3.2), performed sequentially after checking for Fe present as acid volatile sulfides. For the carbonate and oxide fractions, fresh bulk powders are sequentially leached with: (1) 1 M sodium acetate ($C_2H_3NaO_2$) adjusted to pH 4.5 with acetic acid (CH_3COOH) for 48 h at 50 °C to release carbonate iron (Fecarb); (2) dithionite solution (mixture of 50 g L^{-1} sodium dithionite ($Na_2S_2O_4$), 0.2 M sodium citrate ($Na_3C_6H_5O_7{\cdot}H_2O$) and 0.35 M acetic acid) for 2 h to release iron from ferric oxides such as hematite and goethite (Feox); and (3) ammonium oxalate solution (mixture of 0.2 M ammonium oxalate ($C_2H_8N_2O_4$) and 0.17 M oxalic acid ($H_2C_2O_4{\cdot}H_2O$)) for 6 h to extract iron from magnetite (Fe_{mag}). The iron extracted from carbonates, oxides and sulfides are combined to yield the highly reactive pool (Fe_{HR}). This Fe_{HR} pool represents Fe minerals that are reactive toward dissolved sulfide on diagenetic timescales (Canfield et al., 1992; Poulton et al., 2004a). Total iron concentrations (Fe_T) were determined by total digestion with concentrated HF, HNO_3 and $HClO_4$. All Fe extracts were analyzed by Flame Atomic Adsorption Spectroscopy, with repeat analyses yielding RSD's of <5% for all stages.

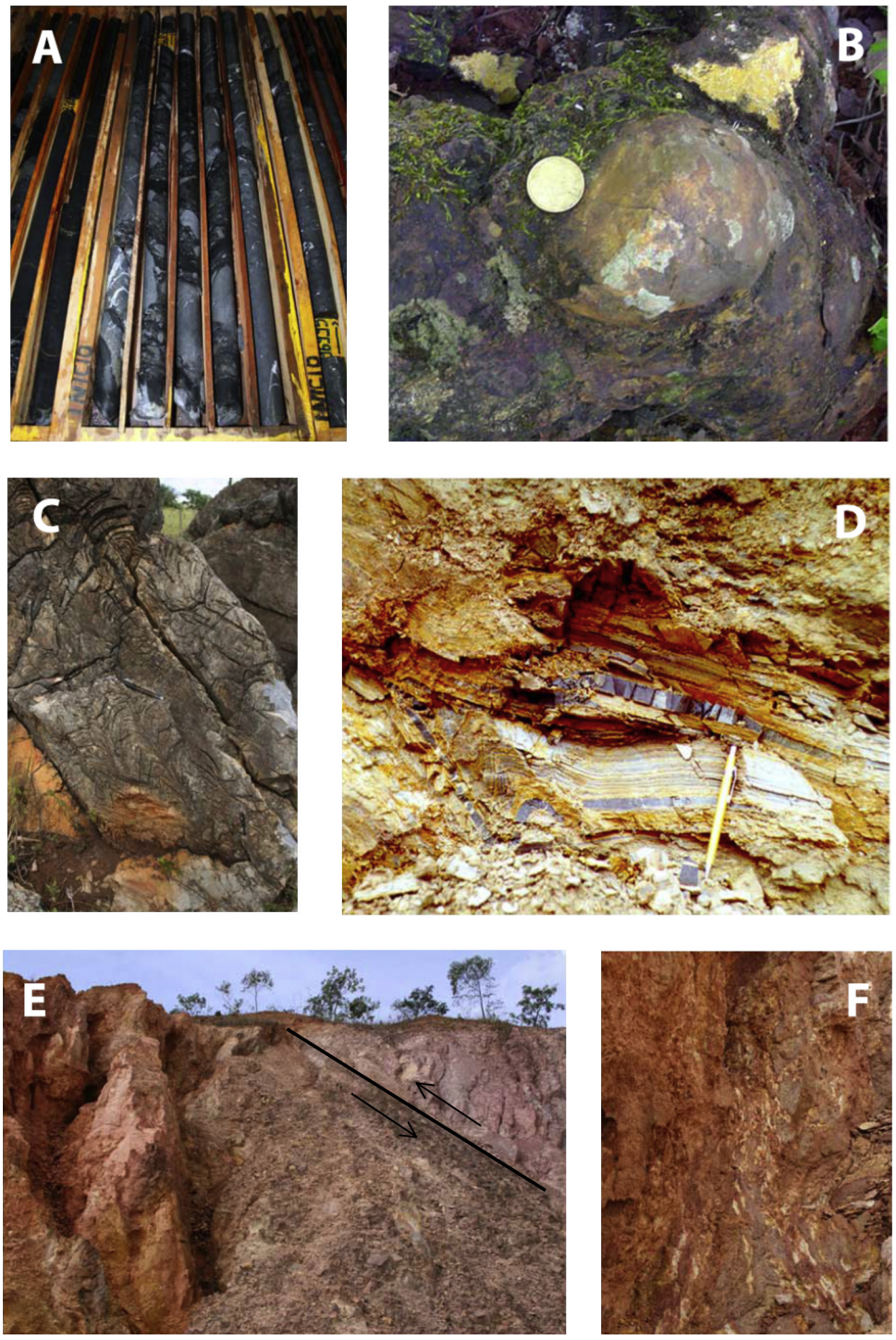

Fig. 3. Photographs of (A) carbonate ice-rafted debris in the organic-rich post-glacial shale of the Morro do Calcário Formation in drill core MASW-01; (B) faceted cobble in silicified shale matrix of the Morro do Calcário Formation near Paracatu, MG, Brazil; (C) *Conophyton* stromatolites from the basal Lagamar Formation above the thrust fault; (D) phosphorite and high-Sr limestone from the Rocinha Formation located below the thrust fault and west of the Vazante mine; (E) thrust fault trace with brown to mauve sandy mylonite to the left and bedded purple shale and siltstone of the upper Rocinha Formation to the right; (F) Close up of clay and quartz-rich mylonite at thrust fault contact.

4. Results

4.1. Re–Os

Results of Re and Os analyses for the Serra do Garrote, Morro do Calcário and Lapa formation shales are reported in Table 1. In the Serra do Garrote samples, Re and Os concentrations ranged from ~1 to 16 ppb, and ~60 to 600 ppt, respectively. The isotopic data show a generally isochronous relationship (Fig. 4A) indicating an age of 1354 ± 88 Ma (n = 8, MSWD = 49). Presuming the isochron age to be accurate, the initial $^{187}Os/^{188}Os$ value (Os_i) of each sample is back-calculated. The reproducibility of Os_i of individual samples in the Serra do Garrote shale (Table 1) suggests minimal post-depositional mobility (Kendall et al., 2009). The Serra do Garrote date presented here is, admittedly, imprecise with a relatively high MSWD value. However, the Os_i from the isochron regression falls

Table 1
Re and Os abundance and isotope data for black shale intervals in the Serra do Garrote, Morro do Calcário and Lapa Formations. Os_i = initial $^{187}Os/^{188}Os$ ratio back-calculated using the isochron age in Fig. 4.

	Sample	Drill hole	Core depth	Re (ppb)	Os (ppt)	$^{187}Re/^{188}Os$	$^{187}Os/^{188}Os$	Os_i
Lapa Fm.	L1	134-86	587.84	0.322 ± 0.008	35.0 ± 0.4	53.34 ± 1.19	1.709 ± 0.003	N/A
	L2	134-86	589.90	0.288 ± 0.008	33.4 ± 0.4	50.73 ± 1.53	1.838 ± 0.007	N/A
	L3	134-86	590.50	0.138 ± 0.008	26.1 ± 0.4	30.4 ± 1.8	1.59 ± 0.01	N/A
	L4	134-86	591.34	0.366 ± 0.008	52.3 ± 0.5	39.05 ± 0.92	1.358 ± 0.006	N/A
Morro do Calcário Fm.	MC1	42-88	803.89	0.435 ± 0.009	31.6 ± 0.1	80.7 ± 1.8	1.86 ± 0.01	0.33
	MC1_dup	42-88	803.89	0.360 ± 0.007	31.5 ± 0.1	67.2 ± 1.5	1.88 ± 0.01	0.6
	MC2	42-88	804.00	0.690 ± 0.014	42.5 ± 0.1	100.0 ± 2.2	2.352 ± 0.003	0.46
	MC3	42-88	804.43	0.334 ± 0.007	31.6 ± 0.1	59.5 ± 1.3	1.46 ± 0.01	0.34
	MC3_dup	42-88	804.43	0.303 ± 0.006	26.9 ± 0.1	65.7 ± 1.4	1.79 ± 0.01	0.54
	MC4	42-88	804.48	0.858 ± 0.017	50.5 ± 0.2	107.0 ± 2.4	2.549 ± 0.01	0.53
	MC4_dup	42-88	804.48	0.831 ± 0.017	62.9 ± 0.2	78.2 ± 1.7	1.911 ± 0.009	0.44
	MC5	42-88	804.50	0.387 ± 0.008	33.5 ± 0.1	67.6 ± 1.5	1.82 ± 0.01	0.54
	MC6	134-86	676.05	3.498 ± 0.014	131.1 ± 0.4	195.2 ± 1.2	4.159 ± 0.004	0.46
	MC6_dup	134-86	676.05	3.485 ± 0.014	132.9 ± 0.4	194.4 ± 1.2	4.323 ± 0.006	0.64
	MC7	134-86	677.40	8.702 ± 0.035	244.4 ± 0.7	296.2 ± 1.8	5.744 ± 0.005	0.21
	MC7_dup	134-86	677.40	8.030 ± 0.032	227.7 ± 0.7	306.8 ± 1.8	6.365 ± 0.009	0.63
	MC8	134-86	680.78	6.137 ± 0.025	213.5 ± 0.6	217.5 ± 1.3	4.539 ± 0.005	0.47
	MC8_dup	134-86	680.78	5.871 ± 0.023	212.3 ± 0.6	207.1 ± 1.2	4.417 ± 0.005	0.54
	MC9	134-86	683.60	4.070 ± 0.016	129.0 ± 0.4	258.3 ± 1.5	5.581 ± 0.006	0.68
	MC10	134-86	691.23	6.570 ± 0.026	184.9 ± 0.6	300.6 ± 1.8	5.993 ± 0.004	0.35
Serra do Garrote Fm.	G1	134-86	824.37	16.02 ± 0.07	578.7 ± 1.2	222.5 ± 1.5	5.257 ± 0.003	0.19
	G1_dup	134-86	824.37	15.63 ± 0.07	588.7 ± 1.2	212.7 ± 1.4	5.209 ± 0.005	0.19
	G2	134-86	824.42	11.56 ± 0.06	370.1 ± 0.7	274.9 ± 2.1	6.468 ± 0.006	0.20
	G2_dup	134-86	824.42	11.72 ± 0.06	356.8 ± 0.7	300.4 ± 2.3	7.017 ± 0.006	0.17
	G3	134-86	824.76	1.093 ± 0.012	60.6 ± 0.1	116.2 ± 1.5	2.724 ± 0.003	0.07
	G3_dup	134-86	824.76	1.038 ± 0.012	80.2 ± 0.2	76.31 ± 1.00	1.844 ± 0.002	0.10
	G4	134-86	825.83	11.97 ± 0.07	355.4 ± 0.7	305.3 ± 2.3	6.892 ± 0.006	−0.07
	G5	134-86	825.86	5.650 ± 0.028	223.5 ± 0.4	189.8 ± 1.3	4.38 ± 0.005	0.06

between values of ~0.12 (chondritic/mantle compositions in the late Mesoproterozoic; Walker et al., 2002a,b) and 1.5 (riverine inputs; Levasseur et al., 1999) that would reasonably be expected for seawater $^{187}Os/^{188}Os$. Such an observation suggests that any post-depositional disturbance is relatively minor. The large uncertainty (~5%) on the age may arise from changes in the initial Os isotopic composition of seawater during deposition (data used to generate Fig. 4A come from samples spreading approximately 1.5 m of section). The changing Os isotopic composition of the source water and minor open-system behavior may also explain the relatively high MSWD value.

Rhenium and Os concentrations in the thick, organic-rich Morro do Calcário shale vary substantially between the two sampled cores, which were drilled ~2.3 km apart. Samples from drill core 42-88 contain between ~0.30 and 0.85 ppb Re and between ~27 and 55 ppt Os, while those from drill core 134-86 are characterized by higher concentrations with ~1–23 ppb Re and ~40–700 ppt Os. The differences are most likely related to environmental and facies variations, as metal abundances in the two cores are broadly correlated with that of total organic carbon, suggesting sedimentary controls on their distribution (Anbar et al., 2007). Sample sets from these two cores can be combined to yield a composite isochron with an age of 1112 ± 50 Ma (n = 16, MSWD = 91; Fig. 4B). Although care was taken to sample the two drill cores from roughly equivalent horizons, we cannot *a priori* assume that these horizons are directly contemporaneous, particularly as the data plot in two distinct positions along the isochron. Furthermore, the samples from drill core 42-88 have very low Re and Os abundances, and therefore may be more readily contaminated by detrital components of the shale (Azmy et al., 2008). Taking only the more metal enriched Morro do Calcário samples from drill core 134-86 results in an imprecise isochron age of 1035 ± 200 Ma (n = 8, MSWD = 150; Fig. 4C) with scatter that is greater than analytical uncertainties. Duplicate analyses of some samples gave minor to moderate differences in $^{187}Re/^{188}Os$ and $^{187}Os/^{188}Os$ and likely reflect variable extents of powder heterogeneity. While neither the composite isochron nor the drill core 134-86 isochron are strong enough to warrant a direct depositional age assignment, it is worth noting that both are statistically identical to the Morro do Calcário Formation's previously assigned Re–Os age (1100 ± 77 Ma; Azmy et al., 2008).

Samples from the thin Lapa Formation shale in core 134-86 have the lowest concentrations of both Re and Os in this study (Table 1), and exhibit a very limited range in $^{187}Re/^{188}Os$ and $^{187}Os/^{188}Os$. Hence, these samples do not define an isochron, and we do not consider the Lapa Formation measurements further.

4.2. C–S

Results for time-series C and S analyses from the Serra do Garrotte, Morro do Calcário and Lapa formations sampled from drill core 134-86 and 42-88 are reported in Table 2 and illustrated in Figs. 5 and 6. In core 134-86 (Fig. 5), where all three shale horizons were collected and analyzed, TOC abundances range widely between 0 and 4 wt.% with highest overall (but variable) abundances in the Morro do Calcário shale and in a singular peak within the Lapa shale. Carbon isotope compositions of Serra do Garrotte samples range between −28 and −31‰, values similar to samples from the base of the Morro do Calcário Formation. Stratigraphically higher in the Morro do Calcário, samples define a trend of ^{13}C enrichment with $\delta^{13}C$ values reaching as high as −22‰. In contrast, organic matter in Lapa Formation samples have relatively constant $\delta^{13}C$ values around −25‰. Sulfur isotope compositions in this core were not measured for the Serra do Garrotte Formation. In the Morro do Calcário, sample $\delta^{34}S$ values range from +10 to −15‰, becoming more depleted in ^{34}S up-section. In contrast, Lapa Formation samples are notably enriched in ^{34}S, ranging from +10 to +35‰, defining a positive excursion that peaks in the most organic-rich horizons.

Morro do Calcário samples from core 42-88 (Fig. 6) were previously studied for biomarker distributions and organic carbon

Table 2
Time-series total organic carbon (TOC) abundances in weight percent; carbon isotopic composition of the organic carbon ($\delta^{13}C$); sulfur isotopic composition of the sulfide sulfur ($\delta^{34}S$); and sulfide sulfur abundance in weight percent (S) of the Serra do Garrote, Morro do Calcário and Lapa Formations in drill core 134-86 as well as the Morro do Calcário Formation of drill core 42-88. Uncertainties do not exceed: TOC and S ±10% of value; $\delta^{13}C \pm 0.15$‰; $\delta^{34}S \pm 0.35$‰. nd = not detected.

	Depth (m) Core 134-86	TOC (wt.%)	$\delta^{13}C$, TOC (‰, VPDB)	$\delta^{34}S$, Sulfide (‰, VCDT)		Depth (m) Core 134-86	TOC (wt.%)	$\delta^{13}C$, TOC(‰, VPDB)		Depth (m) Core 42-88	TOC (wt.%)	$\delta^{13}C$, TOC	S (wt.%)	$\delta^{34}S$, Sulfide(‰, VCDT)
Lapa Fm.	560.70	0.161	−25.83	nd	Serra do Garrote Fm.	822.93	2.39	−30.27	Morro do Calcário Fm.	749.03	0.404	−28.3	0.15	7.49
	561.82	0.2	−24.66	11.91		823.45	2.73	−28.95		752.35	0.156	−25.9	0.42	13.7
	565.40	0.22	−26.02	19.58		824.35	2.07	−28.74		756.20	0.333	−26.0	0.18	5.69
	567.83	0.1	–	11.67		824.73	1.75	−29.74		759.55	0.0797	−26.3	0.017	29.9
	572.64	0.23	−24.37	17.59		825.83	1.61	−30.00		764.47	0.0788	−26.4	0.052	18.8
	575.60	0.19	−24.80	9.62		827.32	1.49	−29.96		769.75	0.0440	−26.3	0.061	12.1
	576.93	nd	nd	20.69		827.47	2.01	−29.62		774.20	0.0336	−26.0	0.0087	14.9
	577.92	0.08	−24.48	27.09		828.75	1.03	−29.39		779.10	–	–	–	–
	579.27	–	−25.23	nd		829.32	0.832	−29.08		783.10	0.0484	−26.1	0.061	27.9
	580.83	0.07	−25.83	nd		831.00	0.906	−29.31		788.15	0.0827	−25.6	1.5	19.7
	582.74	0.1	−25.42	20.93		831.25	0.312	−28.38		793.70	0.314	−26.6	0.68	24.9
	585.00	0.24	−24.66	15.49		832.83	0.585	−28.92		799.10	1.98	−29.1	2.3	24.9
	585.60	0.21	−24.80	16.5		833.73	0.643	−28.63		799.25	1.53	−25.2	1.1	26.7
	585.80	0.12	−25.40	14.48		833.88	0.234	−25.32		799.39	1.72	−25.2	0.0087	23.3
	586.20	0.22	−23.24	19.99		835.29	0.518	−28.64		799.97	0.0410	−24.1	0.85	8.51
	587.84	1.47	−25.06	26.4		836.36	0.375	−28.95		800.12	0.142	−23.6	2.1	30.6
	589.90	1.45	−25.66	30.07		837.00	0.806	−29.31		800.60	1.31	−25.1	0.078	18.4
	590.50	1.5	−25.42	29.13		838.87	0.845	−28.75		801.34	1.05	−25.3	1.0	30.0
	591.34	3.73	−24.84	nd		838.92	0.234	−28.37		802.67	1.69	−25.6	2.3	27.3
	592.23	1	−25.23	30.1		839.58	0.195	−28.31		803.82	0.890	−25.4	1.7	25.2
	593.20	0.44	−24.48	34.69		841.35	0.208	−28.14		804.43	1.79	−25.1	2.2	25.3
	593.28	0.65	–	35.52		841.55	0.26	−28.85		804.63	0.675	−25.2	–	26.5
	593.47	0.46	−24.37	27.02		844.00	0.494	−29.80		806.02	2.45	−26.6	1.2	16.1
	594.04	1.68	−24.85	28.81		844.79	0.455	−30.04		807.75	0.431	−25.6	0.51	27.7
	595.42	1.12	−25.18	26		845.29	1.19	−30.74		808.32	0.750	−26.0	0.61	24.3
	596.20	0.44	−24.88	26.85		846.53	0.844	−30.37		809.12	0.831	−25.4	0.88	23.9
	596.33	–	−25.32	27.18		847.69	3.42	−29.90		810.15	0.420	−25.9	0.56	26.3
	596.85	–	−25.79	28.7		848.00	2.62	−29.76		810.55	1.90	−26.3	3.2	23.0
	597.43	0.13	–	28.86		848.90	2.16	−29.73		811.75	3.03	−25.8	1.0	20.2
	598.10	0.15	−26.02	19.52		850.12	2.4	−29.75		813.05	1.91	−26.3	0.63	16.8
Morro do Calcário Fm.	606.80	nd	nd	23.48		851.15	2.53	−30.12		814.17	1.82	−25.2	1.1	18.2
	607.78	nd	nd	20.33		850.12	2.4	−29.75		814.53	0.479	−25.8	0.27	22.4
	607.84	nd	nd	21.38		851.15	2.53	−30.12		815.08	0.643	–	0.050	14.4
	608.70	nd	nd	nd						816.95	0.507	−25.9	1.3	20.4
	610.52	nd	nd	8.77						818.00	2.09	−27.0	1.7	10.2
	611.58	nd	nd	−1.97						818.23	1.06	−26.9	2.1	15.8
	612.23	1.57	−25.56	14.72						820.20	0.0802	−25.0	nd	nd
	613.13	1.65	−25.76	23.66						825.25	0.221	−12.5	0.25	11.5
	614.27	0.543	−25.74	19.9						830.00	0.0650	−20.2	1.5	–
	616.20	0.596	−21.82	nd						835.40	0.282	−23.1	0.49	9.70

Table 2 (*Continued*)

Depth (m) Core 134-86	TOC (wt.%)	$\delta^{13}C$, TOC (‰, VPDB)	$\delta^{34}S$, Sulfide (‰, VCDT)	Depth (m) Core 134-86	TOC (wt.%)	$\delta^{13}C$, TOC(‰, VPDB)	Depth (m) Core 42-88	TOC (wt.%)	$\delta^{13}C$, TOC	S (wt.%)	$\delta^{34}S$, Sulfide(‰, VCDT)
619.69	0.021	−21.08	nd								
620.09	0.9	−28.99	−1.89								
622.46	1.33	−29.90	3.29								
624.86	1.38	−30.04	−1.83								
627.72	0.484	−24.71	3.2								
628.43	0.578	−26.75	nd								
638.17	3.43	−23.20	−5.84								
638.69	0.431	−25.15	−13.03								
639.38	1.12	−26.11	−2.46								
640.89	0.364	−25.14	nd								
642.05	2.82	−27.07	1.1								
644.05	4.04	−26.43	nd								
648.61	0.382	−23.34	nd								
649.32	0.191	−22.57	1.45								
651.31	0.214	−22.56	nd								
655.02	0.56	−24.48	−4.82								
658.16	1.27	−27.51	5.7								
662.25	3.26	−28.85	5.25								
667.29	0.672	−28.24	nd								
668.73	1.6	−29.07	5.25								
674.09	1.19	−29.03	15.61								
676.12	2.19	−29.73	9.88								
677.55	2.06	−29.37	7.32								
680.82	1.52	–	8.45								
683.69	2.42	−30.06	nd								
688.14	1.29	−29.54	8.26								
691.32	3.82	−29.37	3.15								
696.27	1.91	–	4.01								

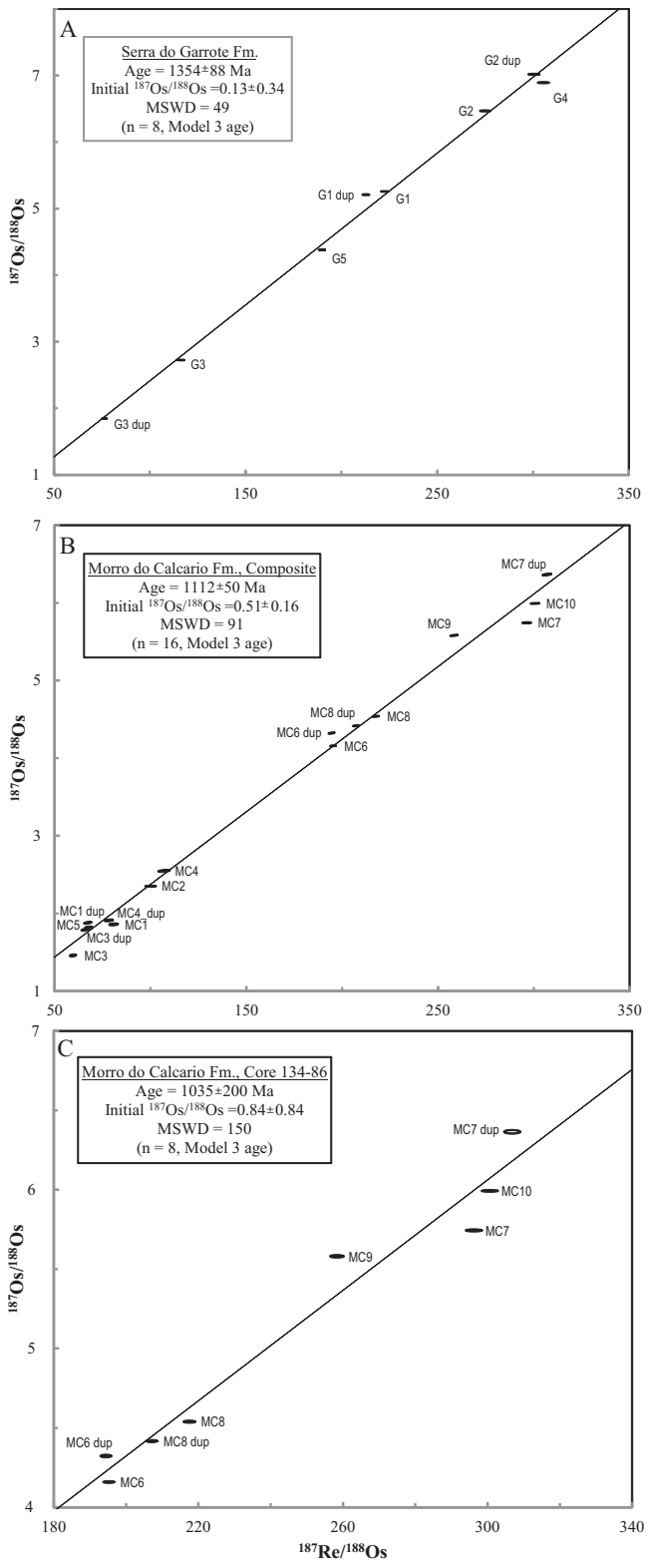

Fig. 4. Re–Os isochrons for: (A) Serra do Garrote Formation samples from drill core 134-86; (B) Morro do Calcário Formation samples from drill core 42-88 and 134-86; (C) Morro do Calcário Formation samples taken only from drill core 134-86.

contents (Olcott et al., 2005). TOC abundances in these samples range up to 3.5 wt.%, with most samples having $\delta^{13}C$ values near to −25‰, regardless of organic carbon content. Sulfur contents are similar to those of organic matter, ranging up to 3 wt.%, but $\delta^{34}S$ values define a significant positive excursion with a progressive 20‰ rise in the lower half of the section to values as high as approximately +30‰, which fall back to around +10‰ in the upper half of the section.

4.3. Fe-speciation

Iron-speciation analyses were conducted on the Morro do Calcário samples from core 42-88 (Fig. 6; Table 3) in order to better understand the redox architecture of the depositional basin and for comparison with environmental interpretations from the previously published biomarker results. Fe_{HR}/Fe_T ratios can be used to distinguish oxic from anoxic water column depositional conditions, whereby values >0.38 provide strong support for anoxic deposition, while values <0.22 suggest oxic depositional water column conditions (Raiswell and Canfield, 1998; Poulton and Raiswell, 2002; Poulton and Canfield, 2011). For samples that show clear evidence for anoxic deposition, Fe–S/Fe_{HR} values >0.7–0.8 suggest euxinic deposition, while values below this threshold suggest anoxic non-sulfidic depositional conditions (Poulton et al., 2004b; Poulton and Canfield, 2011). Fe_{HR}/Fe_T ratios range widely through the formation (Fig. 6). Notably high values for samples at depths <759 m, between 785 and 812 m, and >825 m provide strong evidence for dominantly anoxic deposition across these intervals, perhaps with occasional transitions to oxic deposition from 800 to 812 m (potentially a consequence of fluctuations in the depth of the chemocline). In contrast, low Fe_{HR}/Fe_T from 759 to 785 m and 812 to 825 m depths suggests dominantly oxic water column conditions for these samples, although periodically higher Fe_{HR}/Fe_T ratios suggest the possibility of cycling between oxic and anoxic conditions. To distinguish anoxic non-sulfidic and euxinic deposition, Fe–S/Fe_{HR} ratios are plotted on Fig. 6 for samples which show evidence of anoxic deposition (i.e., $Fe_{HR}/Fe_T > \sim 0.38$). In general, lower Fe–S/Fe_{HR} toward the top and bottom of the section implies anoxic non-sulfidic depositional conditions, while higher values in the middle portion of the section suggests dominantly euxinic conditions.

5. Discussion

Although the Re–Os isochron ages for upper Vazante shales determined previously (Azmy et al., 2008) and in this study are imprecise, they are consistent with a late Mesoproterozoic to earliest Neoproterozoic age assignment. This age for the Vazante Group contrasts with an earlier chemostratigraphic age estimate (Azmy et al., 2001, 2006), which was in part based on the assumption that all the glacial deposits must be from the Neoproterozoic Era.

5.1. Stratigraphic context for a Mesoproterozoic age of the upper Vazante Group

Detrital zircons from the middle of the Serra do Garrote and the top of the Morro do Calcário formations yield U–Pb ages varying from 1505 to 2521 Ma and 1109 to 2466 Ma, respectively; lower in the Serra do Garrote detrital zircon ages vary from 1242 to 3409 Ma (Rodrigues et al., 2012). Taken as maximum depositional ages, these former dates do not contradict the Re–Os ages but do require relatively rapid unroofing and transportation of the zircons. In contrast, younger detrital zircon U–Pb ages from formations of the Vazante Group below the shale horizons (Azmy et al., 2008; Rodrigues et al., 2012) do appear to contradict our Re–Os age estimates. For example, the Rocinha Formation contains zircons as young as 930 Ma and the St. Antônio do Bonito Formation contains zircons with ages as young as ~1000 Ma (Azmy et al., 2008; Rodrigues et al., 2012), suggesting a likely Neoproterozoic age for this part of the succession. In support of this view, Sr isotope compositions of phosphorite samples from the Rocinha Formation (Fig. 3D), with $^{87}Sr/^{86}Sr$ values of

Table 3
Results from the analysis of the Morro do Calcário Formation shale interval in the Mesoproterozoic Vazante Group, drill core 42-88. Iron speciation analyses: All concentrations are in weight% (nd = not detected). FeT = total iron; Fecarb = carbonate iron; Fox = oxide iron; Femag = magnetite iron; Fe-AVS = acid volatile sulfide iron; Fepy = pyrite iron; FeHR = highly reactive iron; Fe–S = Fe-AVS + Fepy.

	Depth (m)	FeT	Fecarb	Feox	Femag	Fe-AVS	Fepy	FeHR	FeHR/FeT	Fe–S/FeHR
Morro do Calcário Fm.	749.03	1.521	0.655	0.196	0.154	nd	0.236	1.241	0.816	0.190
	752.35	2.369	0.856	0.268	0.179	nd	0.601	1.904	0.804	0.316
	756.20	3.116	1.442	0.463	0.305	0.002	0.155	2.365	0.759	0.066
	759.55	2.235	0.324	0.063	0.062	nd	0.072	0.521	0.233	0.138
	764.47	2.132	0.302	0.104	0.061	0.004	0.075	0.542	0.254	0.146
	769.75	2.243	0.725	0.194	0.116	nd	0.094	1.129	0.503	0.083
	774.20	2.221	0.077	0.075	0.030	nd	0.031	0.213	0.096	0.146
	779.10	2.015	0.077	0.038	0.023	nd	0.005	0.143	0.071	0.035
	783.10	0.944	0.527	0.145	0.093	0.002	0.137	0.902	0.956	0.154
	788.15	3.169	0.608	0.129	0.157	nd	1.499	2.393	0.755	0.626
	793.70	0.502	0.359	0.082	0.025	nd	0.001	0.467	0.930	0.002
	799.10	2.301	1.032	0.220	0.307	nd	0.384	1.943	0.844	0.198
	799.25	3.564	0.012	0.031	0.011	nd	2.077	2.131	0.598	0.975
	799.39	2.442	0.011	0.025	0.008	nd	1.344	1.388	0.568	0.968
	799.97	1.717	0.600	0.178	0.265	nd	0.064	1.107	0.645	0.058
	800.12	1.199	0.322	0.079	0.067	nd	0.526	0.994	0.829	0.529
	800.60	4.938	0.007	0.023	0.007	nd	1.069	1.106	0.224	0.967
	801.34	1.542	0.004	0.020	0.007	nd	0.517	0.548	0.355	0.943
	802.67	2.133	0.008	0.027	0.005	nd	0.899	0.939	0.440	0.957
	803.82	3.392	0.118	0.041	0.043	nd	0.996	1.198	0.353	0.831
	804.43	2.521	0.023	0.027	0.001	nd	0.908	0.959	0.380	0.947
	804.63	3.416	1.128	0.245	0.337	0.004	0.193	1.903	0.557	0.104
	806.02	2.174	0.068	0.036	0.026	nd	0.824	0.954	0.439	0.864
	807.75	3.483	0.381	0.101	0.145	nd	0.561	1.188	0.341	0.472
	808.32	2.961	0.160	0.040	0.048	nd	0.653	0.901	0.304	0.725
	809.12	3.319	0.178	0.080	0.064	nd	0.793	1.115	0.336	0.711
	810.15	1.739	0.184	0.069	0.059	nd	0.443	0.755	0.434	0.587
	810.55	4.605	0.233	0.085	0.074	nd	1.674	2.066	0.449	0.810
	811.75	1.802	0.088	0.054	0.044	nd	0.668	0.854	0.474	0.782
	813.05	3.071	0.208	0.072	0.095	nd	0.168	0.543	0.177	0.309
	814.17	2.329	0.148	0.063	0.033	nd	0.814	1.058	0.454	0.769
	814.53	1.858	0.032	0.041	0.013	nd	0.314	0.400	0.215	0.785
	815.08	3.138	1.102	0.291	0.256	0.006	0.693	2.342	0.746	0.298
	816.95	2.082	0.018	0.022	0.002	nd	0.064	0.106	0.051	0.604
	818.00	2.353	0.563	0.128	0.169	nd	0.439	1.299	0.552	0.338
	818.23	0.836	0.278	0.075	0.079	0.007	0.290	0.722	0.864	0.411
	820.20	6.482	0.247	0.076	0.044	nd	1.878	2.245	0.346	0.837
	825.25	0.700	0.381	0.107	0.057	nd	0.085	0.630	0.900	0.135
	830.00	2.768	0.862	0.188	0.196	nd	1.056	2.302	0.832	0.459
	835.40	0.850	0.407	0.088	0.078	nd	0.208	0.781	0.919	0.266

0.70766 (Misi et al., 2007), match those of the Neoproterozoic Bambuí Group to the east on the São Francisco craton. The cap carbonate at the base of that succession is constrained by a Pb–Pb carbonate age of 740 ± 22 Ma (n = 11; MSWD = 0.66; Babinski et al., 2007).

These paradoxical observations are resolved by the presence of a 40–45° oblique-slip reverse fault beneath outcrops of *Conophyton metula Kirichenko* stromatolite in the Lagamar Formation (Fig. 3E). The fault is identified in aerial photographs and in the field by the presence of brown to yellow clay-rich and sandy mylonite overlying thickly bedded purple shale (Fig. 3F). This reverse fault appears to subdivide the Vazante Group into two parts; older sediments assigned to the Vazante Group are thrust above younger carbonates and phosphates in the Rocinha Formation and the St. Antônio do Bonito Formation glacial diamictite (Misi et al., 2010, 2011). Notably, the Vazante Formation (now Group) originally defined by Dardenne (1978) did not include the basal Santo Antônio do Bonito and Rocinha because these units were severely faulted relative to overlying strata. This tectonic transposition explains many of the conflicting chronometric constraints on the Vazante Group and should be expected given the imbrication of thrust nappes to the west and south in highly metamorphosed terrains (Dardenne, 2000). Movement along this reverse fault – initiated by collision of continental blocks during the late-Neoproterozoic (*ca.* 600 Ma) Brasíliano orogeny – places older strata above younger and separates the Vazante Group into at least two distinct tectonic and sedimentary domains. If this interpretation is correct, the basal Vazante Group diamictite would likely be equivalent to the glacial deposits at the base of the Neoproterozoic Bambuí Group, leaving the two glacial deposits above the thrust fault to be the only radiometrically constrained glaciogenic deposits of the Mesoproterozoic Era. The possibility of additional, yet unrecognized, reverse faults in the Vazante Group cannot be discounted, which may explain the slightly younger U–Pb ages observed in detrital zircons in the lower part of the Serra do Garrote Formation (Rodrigues et al., 2012).

5.2. Regional and depositional setting of the Vazante Group

Two different tectonic models have been proposed to explain the accumulation of Vazante Group strata. In one, Vazante sediments are suggested to have been deposited in a rapidly subsiding foreland basin initiated during collision of the BFB with the flat-lying São Francisco craton at *ca.* 790 Ma (Dardenne, 2000). This suggests a Neoproterozoic age for the succession. However, accepting the Re–Os and U–Pb detrital zircon age constraints, as well as the presence of a major reverse fault within the Vazante succession, it is most likely that only the Rocinha Formation and St. Antônio do Bonito diamictite are correlative with Neoproterozoic deposits on the São Francisco craton (Misi et al., 2010, 2011).

In contrast, upper Vazante Group strata that accumulated on a passive margin carbonate platform are of Mesoproterozoic age

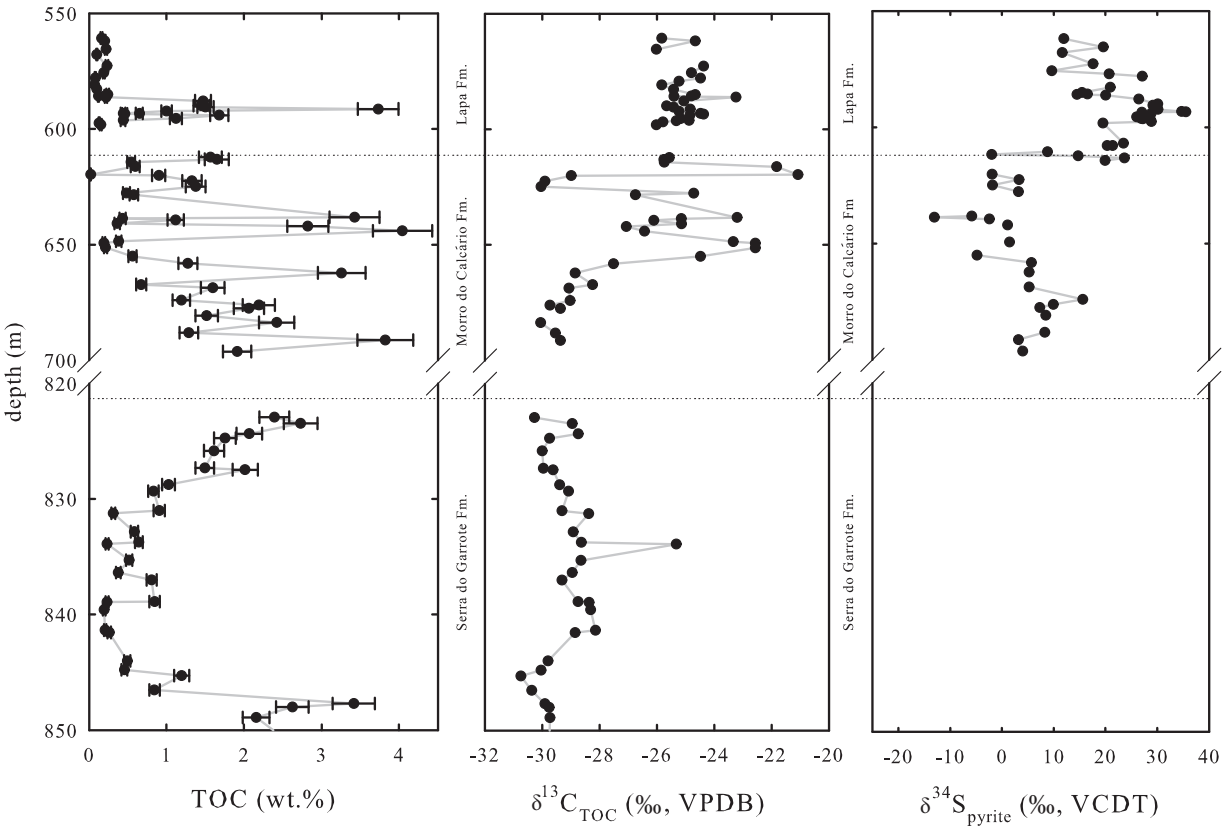

Fig. 5. Time-series elemental and stable isotope compositions of the Serra do Garrote, Morro do Calcário and Lapa Formations (shale intervals only) in the Mesoproterozoic Vazante Group, drill core 134-86 (data available in Table 2), where TOC = total organic carbon.

and likely correlative with the Paranoá Group (Fig. 1) consistent with the interpreted model based on Nd isotopic measurements of detrital grains from a variety of formations across the BFB (Pimentel et al., 2001). The Nd-isotope measurements suggest a likely source of sediments to the Vazante Group was from either the São Francisco craton to the east (T_{DM} ranging from ~2.3 to 1.7 Ga) or the off-shore Goiás Magmatic Arc to the west (T_{DM} ranging from ~1.0 to 1.3 Ga). The initial Nd isotopic compositions of detrital grains from the Serra do Garrote and Serra do Poço Verde formations are identical to those from the nearby Paranoá Group, supporting their direct equivalence (Pimentel et al., 2001). The Paranoá Group lacks direct radiometric constraints but is broadly constrained to between 1200 and 900 Ma (albeit based on stromatolite biostratigraphy; Dardenne and Campos Neto, 1976). The Paranoá Group sits stratigraphically below the Bambuí Group, and glacial deposits have also been observed at its base (Dardenne, 2000). Carbonates in both the Vazante and Paranoá groups reveal relatively little $\delta^{13}C$ variation (Santos et al., 2000; Azmy et al., 2001). The pattern of relatively muted carbon isotope compositions through these successions stands in sharp contrast with Neoproterozoic carbonates of the Bambuí Group which exhibit a striking upsection trend in $\delta^{13}C$ values progressing from as low as −5‰ near its base in a cap carbonate lithofacies to near +15‰ at its top in bituminous limestones (Misi et al., 2007).

Previous biomarker studies of the Morro do Calcário shale (Olcott et al., 2005) interpreted this unit to be syn-glacial based on its appearance between thick carbonate diamictite and ample evidence of ice rafted debris. We currently recognize this organic-rich shale as related to post-glacial transgression with a stratigraphic placement between two carbonate diamictites of different age. Extractable biomarkers (including *n*-alkanes, isoprenoids, steranes and hopanes from shale, carbonate and diamictite) in the Morro do Calcário shale were interpreted to be indigenous to the sediments and reflect a complex microbial ecosystem, including both phototrophic bacteria and eukaryotes living in a stratified ocean with thin or absent sea ice, oxic surface waters and euxinic conditions within the photic zone (Olcott et al., 2005). Our Fe-speciation and S isotope results from the Morro do Calcário shale are consistent with these findings. The partitioning of Fe phases in these ancient sediments suggest that redox conditions in the depositional environment fluctuated on relatively short timescales between anoxic, euxinic and oxic water column conditions as the Morro do Calcário sediments accumulated, supporting the view of initial progressive stratification of the water column followed by generally more expansive ventilation. The dramatic enrichment in ^{34}S of pyrite in the lower part of the sampled interval may thus be interpreted in terms of progressive sulfate-limitation as the water column became increasingly euxinic. Our re-evaluation of this shale as a post-glacial (rather than syn-glacial) deposit, however, complicates our ability to predict aspects of the ice age as they relate to biological productivity and diversity (*cf.* Olcott et al., 2005; Corsetti et al., 2006).

5.3. The Vazante Group in the context of a late Mesoproterozoic world

The upper part of the Vazante Group (as originally described by Dardenne, 2000) is thus far the only radiometrically constrained Mesoproterozoic succession preserving lithological and geochemical evidence of glaciation, so caution about its global significance is warranted. Other studies of late Mesoproterozoic strata indicate that this was a period of a global greenhouse conditions marked by eustatic highstand (Kah et al., 1999, 2012; Gilleaudeau and Kah, 2013). This conundrum may be explained by one of three scenarios: (1) the diamictites of the upper section of the Vazante Group

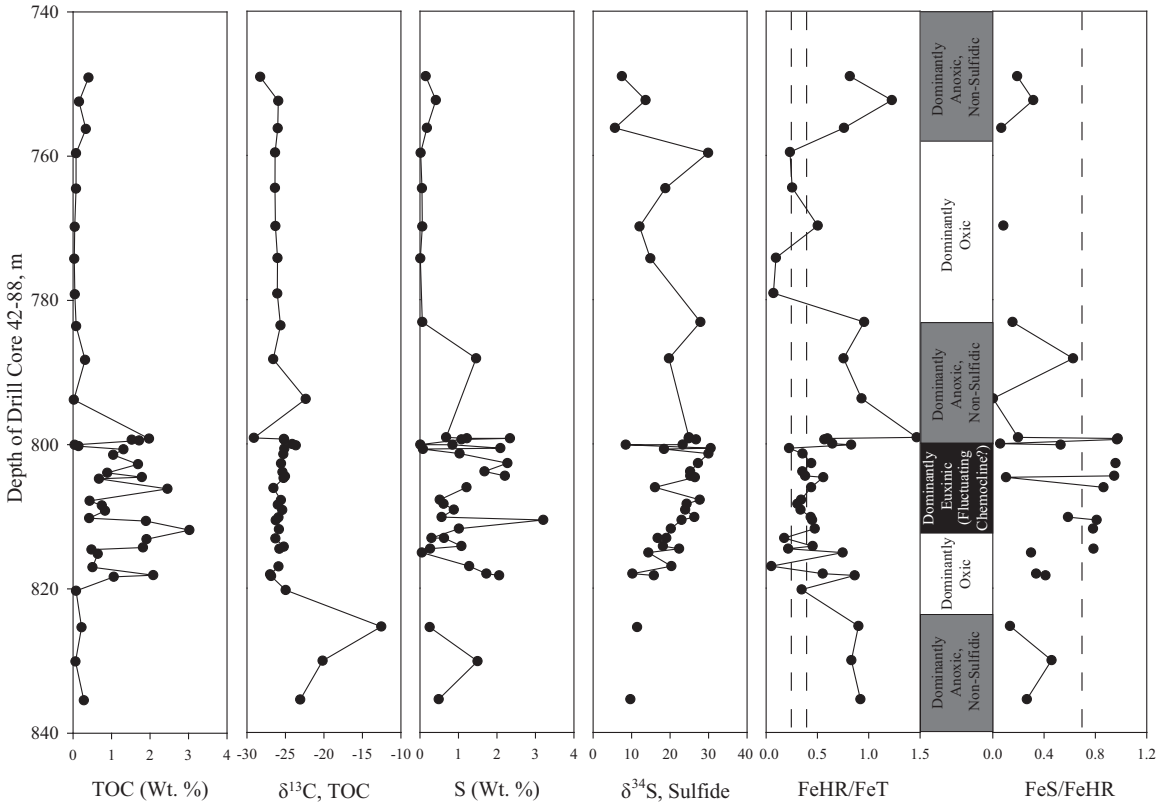

Fig. 6. Time-series elemental and stable isotope compositions of the Morro do Calcário Formation shale interval in the Mesoproterozoic Vazante Group, drill core 42-88 (data available in Tables 2 and 3), where TOC = total organic carbon and S = sulfide-sulfur. Iron speciation data allows identification of deposition from an oxic, anoxic non-sulfidic or euxinic (free sulfide) water column. FeHR = highly reactive iron; FeT = total iron; FeS = pyrite iron. Euxinic conditions are interpreted from FeHR/FeT > 0.38 and FeS/FeHR > ~0.7; anoxic non-sulfidic conditions are recognized from FeHR/FeT > 0.38 and FeS/FeHR < ~0.7; oxic conditions are demonstrated by FeHR/FeT < 0.22. Dashed lines are presented at these threshold values. For all data points, the uncertainty on the measurement is smaller than the symbol.

have been mis-identified as glaciogenic; (2) the Re–Os system has been perturbed or mis-interpreted, and the apparent isochron ages do not reflect the timing of deposition; or (3) the Vazante Group accurately captures a previously unobserved component of the late Mesoproterozoic Earth.

There is strong evidence that units within these strata are the result of multiple discrete glacial events. Glaciation is the most likely mechanism that unites the geology (faceted and striated dropstones along with iron-formation), mineralogy (glendonite) and geochemistry (negative $\delta^{13}C$ excursions) of the upper Vazante Group diamictites. Citing these lines of evidence, this study is not the first to have interpreted glacial strata within the Vazante Group (*cf.* Dardenne, 2001; Azmy et al., 2001, 2006; Brody et al., 2004; Olcott et al., 2005; Misi et al., 2007). However, the Vazante Group diamictites have commonly been interpreted as correlative with Neoproterozic "snowball Earth" deposits found atop the São Francisco craton (Misi et al., 2005) and the conjugate Congo craton (Azmy et al., 2001, 2006). If the Re–Os ages are correct, these correlations will need to be revised. These new data do not warrant altering the interpretation of glacial episodes within the Vazante Group, merely their timing.

The Re–Os system in organic-rich shale has been shown to be fairly robust. It appears unperturbed by low-grade metamorphism (Kendall et al., 2004) and hydrocarbon maturation and expulsion (Creaser et al., 2002) but can be disturbed by surface weathering (Jaffe et al., 2002). The Vazante Group has been exposed to only sub-greenschist faces metamorphism (Babinski et al., 2005; Azmy et al., 2008) in the outcrop region. Furthermore, we sampled from unweathered and well-preserved cores (Azmy et al., 2006). While it is possible for detrital components of the shale to contaminate the hydrogenous Re–Os signatures and thereby influence the isochron ages, we used the Cr^{VI}-H_2SO_4 digestion medium that preferentially attacks the hydrogenous component of the shale over detrital input (Selby and Creaser, 2003; Kendall et al., 2004). Hydrothermal fluid flow can disturb Re–Os systematics but documented cases of remobilization of Re and Os under such conditions have resulted in erroneously *younger*, not older, ages (Kendall et al., 2009). Therefore, even with hydrothermal perturbation, the Serra do Garrote and Morro do Calcário glaciations would not be correlative with the younger, globally distributed Neoproterozoic events.

If the detrital input included organic matter – as suggested for the post-glacial shale of the Morro do Calcário Formation (Marshall et al., 2009) – then preferential digestion of hydrogenous components may result in mixing of authigenic and detrital components and complicated Re–Os systematics. It seems unlikely, however, that such a mixing process would have a consistently wide-spread impact (both temporally and spatially) and result in isochronous relationships. Moreover, the Vazante stata Re–Os dates presented here are in stratigraphic agreement with one another, over a time scale of hundreds of millions of years, and derived from cores drilled approximately 3 km apart. Furthermore, while the Morro do Calcário shale is clearly related to glacial phenomenon, the Serra do Garrote shale is not and thus detrital organic matter contamination through weathering inputs (*cf.* Johnston et al., 2012) should be considerably less significant.

The abundance and wide geographic spread of open marine and epicratonic carbonate platform deposits from the Mesoproterozoic, including the Bangemall Group (Buick et al., 1995), the Turukhansk Group (Knoll et al., 1995; Bartley et al., 2001), the Society Cliffs Formation (Kah et al., 2001) and the Atar Group (Kah et al., 2012)

support the view of a world with globally high sea levels. Notably, the carbon isotope records of these successions are characterized by relatively little variation, predominantly ranging between −4‰ and +4‰, with shifts generally not exceeding 5‰ (Kah et al., 1999; Bartley et al., 2001, 2007; Kah et al., 2012; Gilleaudeau and Kah, 2013). This record stands in stark contrast to the succeeding Neoproterozoic when carbon isotope compositions of marine proxies reveal significant overall ^{13}C enrichments and high amplitude variations (Knoll et al., 1986; Kaufman and Knoll, 1995; Kaufman et al., 1997; Prave et al., 2009; Halverson et al., 2010).

As mentioned above, carbon isotope compositions of marine carbonates in the Vazante Group reveal a moderate spread in $\delta^{13}C$ values, largely falling within the range of −4 to +3‰ (Azmy et al., 2006). This range is consistent with other late Mesoproterozoic successions lacking evidence for glaciation (e.g. Kah et al., 1999). Stratigraphically coherent negative carbon isotope excursions in these successions have recently been explained as a result of relative sea level highstands, which promote anoxia and organic matter remineralization in epicratonic environment (Gilleaudeau and Kah, 2013). In contrast, the upper Vazante Group displays two consistent basin-wide negative shifts of up to 8‰ immediately above the interpreted glacial units (Azmy et al., 2006). Furthermore, the positive S isotope excursion captured in the lower Morro do Calcário shale, which occurs over just 20 m of section (Fig. 6) is similar in magnitude to an event recorded from late Mesoproterozoic bedded sulfates on Baffin Island (Kah et al., 2004). This biogeochemical anomaly is best explained as the result of widespread removal of sulfate (via bacterial sulfate reduction) from an ocean that was relatively sulfate-poor (Canfield, 1998; Kah et al., 2004).

Given the uncertainties of the Re–Os ages presented here and previously (Azmy et al., 2008) and lack of geochronometric constraints in most other late Mesoproterozoic basins, it seems possible that the interval was environmentally variable or that there was a strong temperature gradient between the poles and equator. Paleomagnetic reconstructions place the São Francisco craton at high southern latitudes (45 to over 60° S) in the late Mesoproterozoic (Weil et al., 1998; Tohver et al., 2006), allowing the possibility that the glaciations of the Morro do Calcário and Serra do Garrote formations were local rather than global in extent.

Re–Os age estimates from the Touirist and En Nesoar formations of the Atar Group are statistically identical to the Morro do Calcário Formation (~1100 Ma; Rooney et al., 2010). The similarity of these ages (and Os_i values) as well as their carbon isotopic records have led to the suggestion that these units were deposited coevally atop the West African and São Francisco cratons, respectively (Rooney et al., 2010). Although some aspects of the geochemistry and radiometric constraints are consistent with this hypothesis, the two successions were clearly deposited under conflicting climatic conditions causing other researchers (Kah et al., 2012) to question this correlation. Alternatively, the imprecise age for the Morro do Calcário (Azmy et al., 2008) allow the possibility that Vazante glaciogenic units are younger than the Touirist and En Nesoar formations of the Atar Group. Given the incision of the glacial units into the underlying carbonate platforms (Fig. 2), the Morro do Calcário and Lapa formations may document more substantial sea-level falls following Mesoproterozoic highstands captured elsewhere. Lacking a wider range of sedimentary units from this time period for comparison, it may not be possible to reconcile the Atar Group and other contemporary basins with the Vazante Group until more precise age constraints are available.

6. Conclusions

Based on our geological and radiometric study of Vazante Group strata in south-central Brazil, we conclude that the upper 2/3 of the succession was deposited on a passive margin of the São Francisco craton during the late Mesoproterozoic Era. The Re–Os radiometric ages for the Serra do Garrote (1345 ± 88 Ma; this study) and Morro do Calcário (1100 ± 77 Ma; Azmy et al., 2008) are consistent with previous estimates for upper Vazante strata based on the U–Pb age distributions of detrital zircons. Paleontological and carbon isotopic constraints also support a correlation of the upper section of the Vazante Group (above the Lagamar fault) with the Paranoá Group (also atop the São Francisco Craton), but not the Neoproterozoic Bambuí Group as suggested by earlier authors.

Evidence of two discrete glacial episodes in the upper part of the Vazante stratigraphy is preserved as (1) discrete diamictite horizons bearing both angular and rounded, faceted and striated clasts, sometimes preserved as dropstones in laminated shale; (2) the presence of the cold-water carbonate mineral glendonite within one of the post-glacial shale horizons; (3) Fe-oxide cementation and local accumulation of iron-formation; and (4) negative $\delta^{13}C$ excursion in carbonate overlying the diamictites.

Furthermore, we have identified map and field evidence for an oblique-slip reverse fault that juxtaposes Neoproterozoic glaciogenic strata of the lower Vazante Group (Rocinha and St. Antônio do Bonito) beneath late Mesoproterozoic formations of the upper Vazante Group, including the Serra do Garrote, Morro do Calcário and Lapa units evaluated in this geochemical study. While the fault solves the paradoxical U–Pb maximum depositional ages derived from detrital zircons and the stratigraphic inversion, it also opens up the possibility of other, yet undiscovered, faults within the sequence which may further complicate stratigraphic relationships.

The Vazante Group is unique in the late Mesoproterozoic in that it displays evidence of glaciation in a period generally regarded as a time of greenhouse conditions and globally high sea levels. The glaciations may be regional phenomena as paleo-reconstructions place the São Francisco craton at high southern latitudes during the late Mesoproterozoic Era, but the general lack of open marine successions from this time interval limits our current understanding of this ancient episode of Earth history.

Acknowledgments

The authors wish to thank Kristina Bartlett Brody and Natalie Sievers at the University of Maryland for assistance with analyses and Julio Pinho for help in the field. We also thank Votorantim Metais for access to the drill core samples. This work was partly funded by the National Science Foundation and the National Research Council of Brazil (CNPq 46416/2006-2). Comments from Ruth Schulte and Jim Coleman of the USGS, Julie Bartley, Linda Kah and Geoff Gilleaudeau, as well as two anonymous reviewers appointed by the journal greatly improved this paper. Any use of trade, firm, or product names is for descriptive purposes only and does not imply endorsement by the U.S. Government.

References

Amaral, G., Kawashita, K., 1967. Determinacao da idade do Grupo Bambui pelo metado Rb/Sr. Anais 21st Congresso Brasileiro Geologia Curitiba, Brasil., pp. 214–217.

Anbar, A.D., Duan, Y., Lyons, T.W., Arnold, G.L., Kendall, B., Creaser, R.A., Kaufman, A.J., Gordon, G.W., Scott, C., Garvin, J., Buick, R., 2007. A whiff of oxygen before the Great Oxidation Event? Science 317, 1903–1906.

Azmy, K., Kaufman, A.J., Misi, A., de Oliveira, T.F., 2006. Isotope stratigraphy of the Lapa Formation, São Francisco Basin, Brazil: Implications for Late Neoproterozoic glacial events in South America. Precambrian Res. 149, 231–248.

Azmy, K., Kendall, B., Creaser, R.A., Heaman, L., de Oliveira, T.F., 2008. Global correlation of the Vazante Group, São Francisco Basin, Brazil: Re–Os and U–Pb radiometric age constraints. Precambrian Res. 164, 160–172.

Azmy, K., Veizer, J., Misi, A., de Oliveira, T.F., Sanches, A.L., Dardenne, M.A., 2001. Dolomitization and isotope stratigraphy of the Vazante Formation, Sao Francisco Basin, Brazil. Precambrian Res. 112, 303–329.

Babinski, M., Monteiro, L.S., Fetter, A.H., Bettencourt, J.S., Oliveira, T.F., 2005. Isotope geochemistry of the mafic dikes from the Vazante nonsulfide zinc deposit, Brazil. J. S. Am. Earth Sci. 18, 293–304.
Babinski, M., Vieira, L.C., Trinidade, R.I.F., 2007. Direct dating of the Sete Lagoas cap carbonate (Bambuí Group, Brazil) and implications for the Neoproterozoic glacial events. Terra Nova 19, 401–406.
Bartley, J.K., Kah, L.C., McWilliams, J.L., Stagner, A.F., 2007. Carbon isotope chemostratigraphy of the Middle Riphean type section (Avzyan Formation, Southern Urals, Russia): signal recovery in a fold-and-thrust belt. Chem. Geol. 237, 211–232.
Bartley, J.K., Semikhatov, M.A., Kaufman, A.J., Knoll, A.H., Pope, M.C., Jacobsen, S.B., 2001. Global events across the Mesoproterozoic–Neoproterozoic boundary: C and Sr isotopic evidence from Siberia. Precambrian Res. 111, 165–202.
Bekker, A., Kaufman, A.J., Karhu, J.A., Eriksson, K.A., 2005. Evidence for Paleoproterozoic cap carbonates in North America. Precambrian Res. 137, 167–206.
Birck, J.L., Roy Barman, M., Capmas, F., 1997. Re–Os isotopic measurements at the femtomole level in natural samples. Geostand. Newslett. 21, 19–27.
Brody, K.B., Kaufman, A.J., Eigenbrode, J.L., Cody, G.D., 2004. Biomarker geochemistry of a post-glacial Neoproterozoic succession in Brazil, Geological Society of America Annual Meeting (Abstract), Denver, CO.
Buick, R., Marais, D.J.D., Knoll, A.H., 1995. Stable Isotopic Compositions of Carbonates from the Mesoproterozoic Bangemall Group, Northwestern Australia. Chem. Geol. 123, 153–171.
Canfield, D.E., 1998. A new model for Proterozoic ocean chemistry. Nature 396, 450–453.
Canfield, D.E., Raiswell, R., Westrich, J.T., Reaves, C.M., Berner, R.A., 1986. The use of chromium reduction in the analysis of reduced inorganic sulfur in sediments and shales. Chem. Geol. 54, 149–155.
Canfield, D.E., Raiswell, R., Bottrell, S., 1992. The reactivity of sedimentary iron minerals toward sulfide. Am. J. Sci. 292, 659–683.
Cloud, P., Dardenne, M.A., 1973. Proterozoic age of the Bambui Group in Brazil. Geol. Soc. Am. Bull. 84, 1673–1676.
Cohen, A.S., Coe, A.L., Bartlett, J.M., Hawkesworth, C.J., 1999. Precise Re–Os ages of organic-rich mudrocks and the Os isotope composition of Jurassic seawater. Earth Planet. Sci. Lett. 167, 159–173.
Cohen, A.S., Waters, F.G., 1996. Separation of osmium from geological materials by solvent extraction for analysis by thermal ionization mass spectrometry. Anal. Chim. Acta 332, 269–275.
Corsetti, F.A., Olcott, A.N., Bakermans, C., 2006. The biotic response to Neoproterozoic snowball Earth. Palaeogeogr. Palaeoclimatol. Palaeoecol. 232, 114–130.
Creaser, R.A., Sannigrahi, P., Chacko, T., Selby, D., 2002. Further evaluation of the Re–Os geochronometer in organic-rich sedimentary rocks: A test of hydrocarbon maturation effects in the Exshaw Formation, Western Canada Sedimentary Basin. Geochim. Cosmochim. Acta 66, 3441–3452.
Dardenne, M.A., 1978. Zonação tectônica na borda ocidental do Cráton São Francisco. Anais Congresso Brasileiro de Geologia, vol. 1. Sociedade Brasileira de Geologia, Recife, pp. 299–308.
Dardenne, M.A., 2000. The Brasilia fold belt. In: Cordani, U.G., Milani, E.J., Filho, A.T., Campos, D.A. (Eds.), The Brasilia Fold Belt in Tectonic Evolution of South America. 31st International Geological Congress, Rio de Janeiro. , pp. 231–263.
Dardenne, M.A., 2001. Lithostratrigraphic sedimentary sequences of the Vazante Group. In: IGCP 450 Proterozoic Sediment-Hosted Base Metal Deposits of Western Gondwana (abstract), Belo Horizonte, pp. 48–50.
Dardenne, M.A., Campos Neto, M.C., 1976. Geologia da regiao de Lagamar, Minas Gerais, Congresso Brasileiro de Geologia, 29, Ouro Preto, resumos., pp. 17.
Derry, L.A., Kaufman, A.J., Jacobsen, S.B., 1992. Sedimentary cycling and environmental-change in the Late Proterozoic – evidence from stable and radiogenic isotopes. Geochim. Cosmochim. Acta 56, 1317–1329.
Gilleaudeau, G.J., Kah, L.C., 2013. Carbon isotope records in a Mesoproterozoic epicratonic sea: carbon cycling in a low-oxygen world. Precambrian Res. 228, 85–101.
Halverson, G.P., Wade, B.P., Hurtgen, M.T., Barovich, K.M., 2010. Neoproterozoic chemostratigraphy. Precambrian Res. 182, 337–350.
Hannah, J.L., Bekker, A., Stein, H.J., Markey, R.J., Holland, H.D., 2004. Primitive Os and 2316 Ma age for marine shale: implications for Paleoproterozoic glacial events and the rise of atmospheric oxygen. Earth Planet. Sci. Lett. 225, 43–52.
Harland, W.B., Bidgood, D.E.T., 1959. Palaeomagnetism in some Norwegian sparagmites and the late Pre-Cambrian ice age. Nature 184, 1860–1862.
Hoffman, P.F., Kaufman, A.J., Halverson, G.P., Schrag, D.P., 1998. A Neoproterozoic snowball earth. Science 281, 1342–1346.
Jaffe, L.A., Peucker-Ehrenbrink, B., Petsch, S.T., 2002. Mobility of rhenium, platinum group elements and organic carbon during black shale weathering. Earth Planet. Sci. Lett. 198, 339–353.
Johnston, D.T., Macdonald, F.A., Gill, B.C., Hoffman, P.F., Schrag, D.P., 2012. Uncovering the Neoproterozoic carbon cycle. Nature 483, 320–324.
Kah, L.C., Bartley, J.K., Teal, D.A., 2012. Chemostratigraphy of the Late Mesoproterozoic Atar Group, Taoudeni Basin, Mauritania: muted isotopic variability, facies correlation, and global isotopic trends. Precambrian Res. 200, 82–103.
Kah, L.C., Lyons, T.W., Chesley, J.T., 2001. Geochemistry of a 1.2 Ga carbonate-evaporite succession, northern Baffin and Bylot Islands: implications for Mesoproterozoic marine evolution. Precambrian Res. 111, 203–234.
Kah, L.C., Lyons, T.W., Frank, T.D., 2004. Low marine sulphate and protracted oxygenation of the proterozoic biosphere. Nature 431, 834–838.
Kah, L.C., Sherman, A.G., Narbonne, G.M., Knoll, A.H., Kaufman, A.J., 1999. delta C-13 stratigraphy of the Proterozoic Bylot Supergroup, Baffin Island, Canada: implications for regional lithostratigraphic correlations. Can. J. Earth Sci. 36, 313–332.
Kaufman, A.J., Hayes, J.M., Knoll, A.H., Germs, G.J.B., 1991. Isotopic compositions of carbonates and organic-carbon from upper Proterozoic successions in Namibia-Stratigraphic variation and the effects of diagenesis and metamorphism. Precambrian Res. 49, 301–327.
Kaufman, A.J., Knoll, A.H., 1995. Neoproterozoic variations in the C-isotopic composition of seawater – stratigraphic and biogeochemical implications. Precambrian Res. 73, 27–49.
Kaufman, A.J., Knoll, A.H., Narbonne, G.M., 1997. Isotopes, ice ages, and terminal Proterozoic earth history. Proc. Natl. Acad. Sci. U.S.A. 94, 6600–6605.
Kendall, B., Creaser, R.A., Selby, D., 2006. Re–Os geochronology of postglacial black shales in Australia: constraints on the timing of Sturtian glaciation. Geology 34, 729–732.
Kendall, B., Creaser, R.A., Ross, G.M., Selby, D., 2004. Constraints on the timing of Marinoan Snowball Earth glaciation by Re-187–Os-187 dating of a Neoproterozoic, post-glacial black shale in Western Canada. Earth Planet. Sci. Lett. 222, 729–740.
Kendall, B., Creaser, R.A., Gordon, G.W., Anbar, A.D., 2009. Re–Os and Mo isotope systematics of black shales from the Middle Proterozoic Velkerri and Wollogorang Formations, McArthur Basin, northern Australia. Geochim. Cosmochim. Acta 73, 2534–2558.
Kennedy, M.J., 1996. Stratigraphy, sedimentology, and isotopic geochemistry of Australian Neoproterozoic postglacial cap dolostones: deglaciation, delta C-13 excursions, and carbonate precipitation. J. Sediment. Res. 66, 1050–1064.
Kennedy, M.J., Runnegar, B., Prave, A.R., Hoffmann, K.H., Arthur, M.A., 1998. Two or four Neoproterozoic glaciations? Geology 26, 1059–1063.
Kirschvink, J.W., 1992. Late Proterozoic low-latitude global glaciations: the Snowball Earth. In: Schopf, J.W., Klein, C. (Eds.), The Proterozoic Biosphere. Cambridge University Press, Cambridge, pp. 51–52.
Knoll, A.H., Hayes, J.M., Kaufman, A.J., Swett, K., Lambert, I.B., 1986. Secular variation in carbon isotope ratios from upper Proterozoic successions of Svalbard and East Greenland. Nature 321, 832–838.
Knoll, A.H., Kaufman, A.J., Semikhatov, M.A., 1995. The carbon-isotopic composition of Proterozoic carbonates: Riphean successions from northwestern Siberia (Anabar Massif, Turukhansk uplift). Am. J. Sci. 295, 823–850.
Levasseur, S., Birck, J.-L., Allègre, C.J., 1999. The osmium riverine flux and the oceanic mass balance of osmium. Earth Planet. Sci. Lett. 174, 7–23.
Ludwig, K., 2012. User's manual for Isoplot version 3.75-4.15: a geochronological toolkit for Microsoft. Excel Berkley Geochronological Center Special Publication No. 5.
Marshall, A.O., Corsetti, F.A., Sessions, A.L., Marshall, C.P., 2009. Raman spectroscopy and biomarker analysis reveal multiple carbon inputs to a Precambrian glacial sediment. Org. Geochem. 40, 1115–1123.
Misi, A., Azmy, K., Kaufman, A.J., Oliveira, T.F., Pinho, J.M., Sanches, A.L., 2010. Metallogenic and phosphogenic events in the intracratonic and passive-margin Proterozoic basins of the São Francisco Craton: The Bambuí/Una and Vazante Groups. VII South American Symposium on Isotope Geology, Brasilia, DF. Extended Abstracts.
Misi, A., Azmy, K., Kaufman, A.J., Oiveira, T.F., Pinho, J.M., Sanches, A.L., 2011. High resolution chemostratigraphy and Re–Os ages of organic shales of the Vazante Group (Minas Gerais, Brazil): Implications for mineral exploration modelling. In: XIV Congreso Latino Americano de Geologia, Medellin. Memorias, vol. 1, pp. 410–411.
Misi, A., Iyer, S.S.S., Coelho, C.E.S., Tassinari, C.C.G., Franca-Rocha, W.J.S., Cunha, I.D., Gomes, A.S.R., de Oliveira, T.F., Teixeira, J.B.G., Filho, V.M.C., 2005. Sediment hosted lead–zinc deposits of the Neoproterozoic Bambui Group and correlative sequences, Sao Francisco Craton, Brazil: a review and a possible metallogenic evolution model. Ore Geol. Rev. 26, 263–304.
Misi, A., Kaufman, A.J., Veizer, J., Powis, K., Azmy, K., Boggiani, P.C., Gaucher, C., Teixeira, J.B.G., Sanches, A.L., Iyer, S.S.S., 2007. Chemostratigraphic correlation of neoproterozoic successions in South America. Chem. Geol. 237, 143–167.
Olcott, A.N., Sessions, A.L., Corsetti, F.A., Kaufman, A.J., de Oliviera, T.F., 2005. Biomarker evidence for photosynthesis during Neoproterozoic glaciation. Science 310, 471–474.
Pimentel, M.M., Dardenne, M.A., Fuck, R.A., Viana, M.G., Junges, S.L., Fischel, D.P., Seer, H.J., Dantas, E.L., 2001. Nd isotopes and the provenance of detrital sediments of the Neoproterozoic Brasilia Belt, central Brazil. J. S. Am. Earth Sci. 14, 571–585.
Pinho, J.M.M., Dardenne, M.A., 1994. Caracterização da Falha de Lagamar, NW de Minas Gerais. Abstracts, 38th Brazilian Geological Congress, Sociedade Brasileira de Geologia, Camboriú, SC., pp. 246–247.
Poulton, S.W., Canfield, D.E., 2005. Development of a sequential extraction procedure for iron: implications for iron partitioning in continentally derived particulates. Chem. Geol. 214, 209–221.
Poulton, S.W., Raiswell, R., 2002. The low-temperature geochemical cycle of iron: from continental fluxes to marine sediment deposition. Am. J. Sci. 302, 774–805.
Poulton, S.W., Canfield, D.E., 2011. Ferruginous conditions: a dominant feature of the ocean through Earth's history. Elements 7, 107–112.
Poulton, S.W., Krom, M.D., Raiswell, R., 2004a. A revised scheme for the reactivity of iron (oxyhydr)oxide minerals towards dissolved sulfide. Geochim. Cosmochim. Acta 68, 3703–3715.
Poulton, S.W., Fralick, P.W., Canfield, D.E., 2004b. The transition to a sulphidic ocean ~1.84 billion years ago. Nature 431, 173–177.
Prave, A.R., Fallick, A.E., Thomas, C.W., Graham, C.M., 2009. A composite C-isotope profile for the Neoproterozoic Dalradian Supergroup of Scotland and Ireland. J. Geol. Soc. London 166, 845–857.

Raiswell, R., Canfield, D.E., 1998. Sources of iron for pyrite formation in modern sediments. Am. J. Sci. 298, 219–245.
Ravizza, G., Turekian, K.K., 1989. Application of the Re-187–Os-187 System to Black Shale Geochronometry. Geochim. Cosmochim. Acta 53, 3257–3262.
Rodrigues, J.B., Pimentel, M.M., Buhn, B., Matteini, M., Dardenne, M.A., Alvarenga, C.J.S., Armstrong, R.A., 2012. Provenance of the Vazante Group: new U–Pb, Sm–Nd, Lu–Hf isotopic data and implications for the tectonic evolution of the Neoproterozoic Brasilia Belt. Gondwana Res. 21, 439–450.
Rooney, A.D., Selby, D., Houzay, J.P., Renne, P.R., 2010. Re–Os geochronology of a Mesoproterozoic sedimentary succession, Taoudeni basin, Mauritania: implications for basin-wide correlations and Re–Os organic-rich sediments systematics. Earth Planet. Sci. Lett. 289, 486–496.
Santos, R.V., de Alvarenga, C.J.S., Dardenne, M.A., Sial, A.N., Ferreira, V.P., 2000. Carbon and oxygen isotope profiles across Meso-Neoproterozoic limestones from central Brazil: Bambui and Paranoa groups. Precambrian Res. 104, 107–122.
Schrag, D.P., Berner, R.A., Hoffman, P.F., Halverson, G.P., 2002. On the initiation of a snowball Earth. Geochem. Geophys. Geosyst. 3 (6), 1–21.
Selby, D., Creaser, R.A., 2003. Re–Os geochronology of organic rich sediments: an evaluation of organic matter analysis methods. Chem. Geol. 200, 225–240.
Shirey, S.B., Walker, R.J., 1995. Carius tube digestion for low-blank rhenium–osmium analysis. Anal. Chem. 67, 2136–2141.
Tohver, E., D'Agrella, M.S., Trindade, R.I.F., 2006. Paleomagnetic record of Africa and South America for the 1200–500 Ma interval, and evaluation of Rodinia and Gondwana assemblies. Precambrian Res. 147, 193–222.
Walker, R.J., Horan, M.F., Morgan, J.W., Becker, H., Grossman, J.N., Rubin, A.E., 2002a. Comparative ^{187}Re–^{187}Os systematics of chondrites: implications regarding early solar system processes. Geochim. Cosmochim. Acta 66, 4187–4201.
Walker, R.J., Prichard, H.M., Ishiwatari, A., Pimentel, M., 2002b. The osmium isotopic composition of the convecting upper mantle deduced from ophiolite chromites. Geochim. Cosmochim. Acta 66, 329–345.
Walter, M.R., Veevers, J.J., Calver, C.R., Gorjan, P., Hill, A.C., 2000. Dating the 840–544 Ma Neoproterozoic interval by isotopes of strontium, carbon, and sulfur in seawater, and some interpretative models. Precambrian Res. 100, 371–433.
Weil, A.B., Van der Voo, R., Mac Niocaill, C., Meert, J.G., 1998. The Proterozoic supercontinent Rodinia: paleomagnetically derived reconstructions for 1100 to 800 Ma. Earth Planet. Sci. Lett. 154, 13–24.